MONITORING OF LAND-COVER MOISTURE USING MULTI-TEMPORAL SAR IMAGES

Boyeol Yoon, Kwangjae Lee, Younsoo Kim, Yongseung Kim

Korea Aerospace Research Institute, 45 Eoeun-dong, Youseong-Gu, Daejeon, 305-333, Korea
byoon@kari.re.kr, kjlee@kari.re.kr, younsoo@kari.re.kr, yskim@kari.re.kr

ABSTRACT:

SAR image is not dependent on the weather condition and Sun's electromagnetic energy. But geometric distortions exist in almost all radar image, it need to be correction. The Radarsat-1 SAR images are used to monitoring of moisture acquired in May 1/1998 and May 25/1998. Radarsat-1 C band data is sensitive on moisture condition. Study area is located in Non-san site. It is made up almost agricultural area and a little of forest area. In May, Rice-planting is started in the midland of Korea. So moisture condition is undergoing many changes. Forest area need to be terrain effect removal for accurately results because it is included in layover, shadow, and so on. Results of land-cover moisture condition map are useful tool for fields of agriculture, forestry industry, and disaster.

KEY WORDS: SAR, Radarsat-1, Monitoring, Land-cover moisture condition

1. INTRODUCTION

Recently, Satellite applications are extended to many fields for many years. In August, 1978, the SEASAT-A SAR provided one of the earliest demonstrations of radar's response to soil moisture on a large-area scale (100km by 100km). Conceptually, if the radar backscatting coefficient of terrain is sensitive to several scene variables, then it is necessary to use multiple radar channels(different wavelengths, incident angles, polarization configurations). Another alternative is to use multiple temporal observations, in order to possibly estimate the scene variables of interest with acceptable accuracy. SAR data will be complementary with optical data in the future.

Current research aims to use L- and C-band observations to simultaneously estimate both soil moisture and vegetation biomass of vegetation covered areas, thereby providing more accurate soil moisture maps over a wide range of cover conditions (Ryerson, Robert A., 1998)

This study was conducted to measure the potential of land cover moisture and change detection for short term. Soil moisture analysis can be extended to disaster fields for heavy rains investigation in every from summer to autumn in Korea.

The main aim of this paper is to present the results of this study to the practical use for a local government official, end user, and another application fields for public applications.

2. METHODS

2.1 Study Area and Data sets

The study area (Central coordinate: 127° 11′ 08.16″ E, 36° 12′ 06.30″ N) which is about 25km by 40km and is located in Non-san in the midland of Korea. The land cover consists mainly agricultural lands and forest area. To generate the Digital Elevation Model (DEM), the nine 1:25,000 digitalmap is used.

The Radarsat-1 SAR Fine 5 mode SLC data is 6.25m spatial resolution. Radarsat-1 data is C band (5.6cm, 5.3GHz) and HH polarization. Image data is acquired on May 1, 1998 and May 25, 1998. In Korea, every year in May is irrigated in agricultural area.

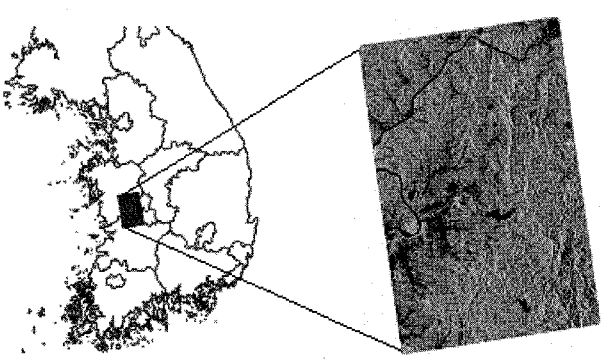

Figure 1. Study area (Radarsat F5 mode)

2.2 Radiometric calibration

Each pixel in the output data is represented by one (or two) digital numbers (DN) which represent the magnitude of the detected pixel data (or the value of each I and Q component for SLC data). The scaling which was applied to the product during processing is described in the CEOS Radiometric Data Record. The following describes how the pixel DNs can be converted to beta naught (β^0) or radar brightness values by extraction and application of the scaling information. Conversion of DNs to radar backscatter coefficient (sigma naught), σ^0, additionally requires knowledge of the incidence angles over the image swath. The conversion from beta naught to sigma naught as a function of pixel incidence angle is described.

$$\beta^0{}_j = 10 * \log_{10}\left[\left(DN_j^{\,2} + A3\right) / A2_j\right] dB \qquad (1)$$

where $A2_j$ is the scaling gain value for the j th. pixel, and A3 is the fixed offset. A3 is obtained directly from scaling offset in the Radiometric Data Record. $A2_j$ is obtained by linear interpolation of the gain values (lookup table) given in output scaling LUT values of the Radiometric Data Record.

$$\sigma^0{}_j = \beta^0{}_j + 10\log_{10}\left(\sin I_j\right) dB \qquad (2)$$

where I_j is the incidence angle at the j th. range pixel. This formula assumes that the earth is a smooth ellipsoid at sea level.

Data required for calculating the incidence angle for any given pixel in the image range line are available in the CEOS record. Given these data, a relatively straightforward approximation to the incidence angle can be performed. For scene products the resulting error in conversion from beta nought to sigma nought resulting from the approximation should be less than 0.4 dB.

Calculate the slant range for each ground range increment of the output scaling LUT. From the Processing Parameter Record: 6 values of slant range for each ground range (SRGR) coefficients [srgr_coef (1-6)].

1st SRGR coeff = a	$a = 8.4087600 \cdot 10^{5}$
2nd SRGR coeff = b	$b = 3.3333325 \cdot 10^{-1}$
3rd SRGR coeff = c	$c = 6.0235465 \cdot 10^{-7}$
4th SRGR coeff = d	$d = -2.4054597 \cdot 10^{-13}$
5 th SRGR coeff = e	$e = -1.1672899 \cdot 10^{-19}$
6 th SRGR coeff = f	$f = 1.9135056 \cdot 10^{-25}$

For SLC products, the slant range pixel spacing, we assume dRs is pixel spacing. For detected products arranged near range pixels first, find the slant range for the j th. pixel from:

$$RS_j = a + j \cdot dRg \cdot b + (j \cdot dRg)^2 \cdot c + (j \cdot dRg)^3 \cdot d + (j \cdot dRg)^4 \cdot e + (j \cdot dRg)^5 \cdot f \qquad (3)$$

For SLC products arranged near range first: RSj = a + dRs·j. For detected products having far range pixels first, calculate the slant range for the j th. pixel from:

$$RS_j = a + j \cdot dRg \cdot b + (j \cdot dRg)^2 \cdot c + (j \cdot dRg)^3 \cdot d + (j \cdot dRg)^4 \cdot e + (j \cdot dRg)^5 \cdot f \qquad (4)$$

For SLC products arranged far range first: RSj = a + dRs·k.
where k = n_data_pixel (the number of data pixels) – j.

The incidence angle for the j th. pixel is given by:

$$I_j = \arccos\left[\frac{\left(h^2 - (RS_j)^2 + 2 \cdot r \cdot h\right)}{2 \cdot RS_j \cdot r}\right] \qquad (5)$$

where r is earth radius and h is satellite altitude (Shepherd, N., 2000).

2.3 Terrain correction

SAR systems measure very exactly the slant-range distances between the SAR sensor and the corresponding illuminated object on the ground. Sometimes these measurements differ from the actually interesting parameters. In case of steep mountainous area, foreshortening, layover, shaded effects is appeared. For this errors correcting, terrain correction is applied for this section.

To calculate the radar brightness for each DEM element, the corresponding image pixels have to be integrated. The radar brightness $\overline{\beta}$ is then given by

$$\overline{\beta} = \frac{1}{n}\sum_{i=1}^{a}\sum_{j=1}^{b}\beta_{i,j} \qquad with\ a+b=n \qquad (6)$$

where I and j denote image coordinates and n is the number of integrated pixels. This method guarantees that the integrated backscatter intensity measured for each pulse is preserved throughout the geocoding process (Löw, A., Mauser, W., 2003).

To compensate for the changing scatting area caused by rugged terrain, we calculate the projection angle ψ proposed by from the local imaging geometry. It is defined as the complementary angle to the smallest angle between the surface normal and the image plane.

The terrain corrected radar backscattering coefficient σ^0 is related to the radar brightness as

$$\sigma^0 = \overline{\beta}\cos\psi \qquad (7)$$

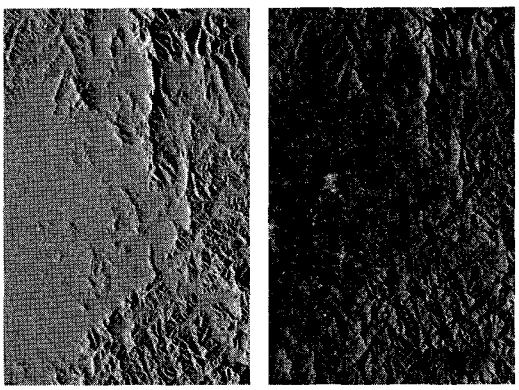

(a) (b)

Figure 2. (a) local incidence angle, (b) corrected image

2.4 Change Detection

In differencing, changes in radar backscatter are measured by subtracting the intensity values, pixel per pixel, between two dates. In ratioing, changes are measured by dividing the intensity values, pixel per pixel, and are conveniently expressed in dB. SAR intensities are assumed to be gamma distribution.

Positive values mean that the first channel of has a higher backscatter than the second channel. Negative values mean the opposite. Zero values mean that there is no difference. To discriminate between changes, two thresholds can be set for positive and negative values. The thresholds are also dB values.

For change detection operation, it is important that the input channels be well registered. Otherwise, the difference image produces a lot of errors.

SAR images contain a lot of speckle-noise that can result in a noisy difference image. Therefore filter can be selected. Both work on the resulting difference image in dB values. Kuan filter is extended Kuan minimum-mean-square-error filter. This filter smooths the noise more accurately and so gives a more complete view of the changes.

The thresholds on the SAR difference image will indicate the pixels that contain a radar-cross-section that is larger than the threshold value. Because radar-cross-sections are often given in dB, this is also the quantity for the thresholds. The indicated pixels are the detected changes in radar-cross-section.

3. RESULTS AND DISCUSSION

Preprocessing results is revealed that backscattering coefficient distribution is from -79.68dB to 4.68dB in May 1 and from -77.64dB to 4.68dB in May 25. By visual interpretation, separated into two kinds of Agricultural areas (irrigated area, non irrigated area) and then, each area is sampled 20 points for used to reference data of threshold values of change detection (Figure 3).

In case of non irrigated area is estimated from -11dB to -7dB in May 1, then after 24 days, values of from -10dB to -6.5dB in May 25. As young rice plant growing, backscattering coefficient is resulted increasing.

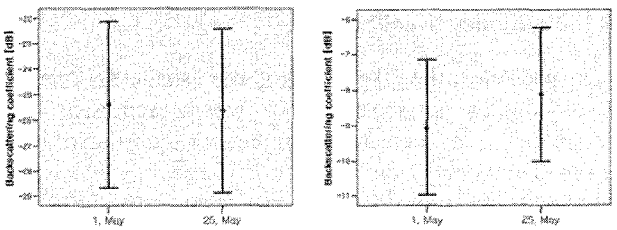

Figure 3. σ^0 variation of agricultural area
(a) Irrigation area, (b) non irrigated area

In change detection differential image is generated backscattering coefficient difference between two dates. Positive and negative values are determined by threshold values criterion. In this results, negative values is indicated decrease of backscattering coefficient, i.e. because irrigated site is showed intensity values lower. In case of positive, this case is higher backscattering coefficient by young rice plant growing or drying soil condition from weather or moisture down from the other effects. As change detection degree, differential image is graded into three parts. Red mark is indicated large change backscattering coefficient (above 9dB). Mainly that area is irrigation area (negative image) or dry out area (positive area). Green mark is medium change is about from 4dB to 8dB in land cover. This area is distributed around agriculture and ridge in mountain. Blue mark is indicated slight backscattering coefficient change (below 3dB). Slight change area is hardly negative image but it is widely distributed in positive image.

4. CONCLUSIONS

Backscattering coefficient of SAR data is useful to over the land cover analysis in this study. Different from optical image, SAR data will be extended to many fields after many new technique and algorithm..

As a result of moisture change detection of SAR data, error factors are related to accuracy. Especially, slight backscattering coefficient variation is almost noise in this paper. Though spatial resolution limitation is exist, a variety factors are considered in data processing for error detection removal. After from now, error factors need to be modified and researched for actually practice through our world.

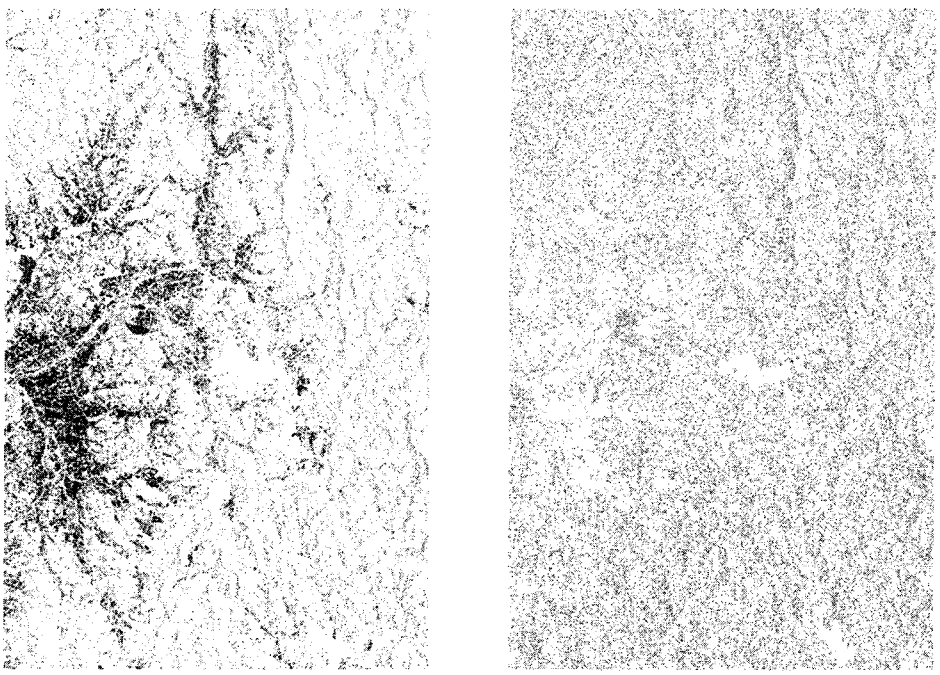

Negative image　　Positive image

Figure 4. Change detection differential image
(■ : large change ■ : medium change ■ : slight change)

5. REFERENCES

Chakaborty, N., Manjunath, K.R., Panigraphy, S., Kundu, N., Parihar, J.S., 2005, Rice crop parameter retrieval using multi-temporal, multi-incidence angle Radarsat SAR data., ISPRS J. Photogramm. Remote Sensings. 59, pp.310-322.

E.J.M. Rignot and J.J. van Zyl. (1993). Change detection techniques for ERS-1 SAR data, IEEE Trans. Geosci Remote Sensing 31(4), pp.896-906.

Löw, A., Mauser, W., 2003, Generation of geometrically and radiometrically terrain corrected ScanSAR images, Geoscience and Remote Sensing Symposium, IGARSS '03. Proceedings. pp.3995- 3997.

Rignot, E.J.M., van Zyl, J.J, 1993, Change detection techniques for ERS-1 SAR data, IEEE Trans. Geosci. Remote Sensing 31(4), pp.896-906.

Ryerson, Robert A., 1998, Maunal of remote sensing, John Wiley & Sons, Inc.

Shepherd, N., 2000, Extraction of Beta Nought and Sigma Nought from RADARSAT CDPF Products Rev. 4. Report No. AS97-5001, ALTRIX Systems Ltd. for the Canadian Space Agency. Ottawa, ON.

Townsend, P.A., 2001, Mapping Seasonal Flooding in Forested Wetlands Using Multi-Temporal Radarsat SAR, PE&RS 67(7), pp.857-864..

Wickle, A.J., Jackson, T.J., Wood, E.F., 2001 Multitemporal monitoring of soil moisture with RADARSAT SAR during the 1997 Southern Great Plains hydrology experiment, Int. J. Remote Sensing, 22(8), pp. 1571-1583.